Chemistry–A European Journal
Communication
doi.org/10.1002/chem.202103525
Chemistry Europe
European Chemical Societies Publishing
www.chemeurj.org

Masked Amino Trimethyl Lock (H_2N-TML) Systems: New Molecular Entities for the Development of Turn-On Fluorophores and Their Application in Hydrogen Sulfide (H_2S) Imaging in Human Cells

Claire Cheyenne Jimidar,[a] Jörg Grunenberg,[a] Bianka Karge,[b, c] Hazel Leanne Sarah Fuchs,[b, c] Mark Brönstrup,[b, c] and Philipp Klahn*[a]

Abstract: Masked trimethyl lock (TML) systems as molecular moieties enabling the bioresponsive release of compounds or dyes in a controlled temporal and spatial manner have been widely applied for the development of drug conjugates, prodrugs or molecular imaging tools. Herein, we report the development of a novel amino trimethyl lock (H_2N-TML) system as an auto-immolative molecular entity for the release of fluorophores. We designed **Cou-TML-N_3** and **MURh-TML-N_3**, two azide-masked turn-on fluorophores. The latter was demonstrated to selectively release fluorescent MURh in the presence of physiological concentrations of the redox-signaling molecule H_2S in vitro and was successfully applied to image H_2S in human cells

Controlled molecular release of effector or reporter molecules in a temporal and spatial manner is of great importance for the development of prodrugs, drug conjugates or bioresponsive molecular imaging tools.[1–5] The controlled release of a cytotoxin from extracellular-targeted anticancer drug conjugates at its target side can reduce systemic adverse effects.[6–9]

Similarly, antimicrobial payloads from extracellular-targeted, antimicrobial drug conjugates, such as siderophore- or antimicrobial peptide-based drug conjugates often need to be released in order to bind their biological targets efficiently.[5,7,10] Furthermore, prodrug strategies including enzymatically removable masking groups can reduce adverse effects or improve pharmacokinetic properties of a drug.[11–14] In addition, the installation of enzymatically cleavable, auto-immolative masking groups in fluorescent dyes leads to quenched or reduced fluorescence, that can be subsequently turned-on upon conversion by a specific enzyme.[15,16] In this context, a highly versatile and robust molecular system that can be employed for the release of molecules in a temporal and spatial manner is the "trimethyl lock" (TML) system, which is based on the high lactonization reactivity of Type **A** trimethyl-substituted *ortho*-hydroxy dihydro cinnamic acid derivatives (Scheme 1).[1] The three pendant methyl groups induce strong steric repulsion and tremendously enhance lactonization rate by a factor of 10^{11} compared to the unsubstituted systems.[17]

The lactonization reactivity can be locked through the installation of thiol responsive, photo responsive, electrochemically or enzymatically cleavable masking groups as triggers for the release of bioactive compounds or reporter groups attached via esters, thioester or amides to the carboxylate function of the TML.[1,2] To date, TMLs have been chemically adapted for the release of compounds by esterases, phosphatases, oxido reductases, nitro reductases and cytochrome P450 monooxygenases, which led to a variety of applications in the design of

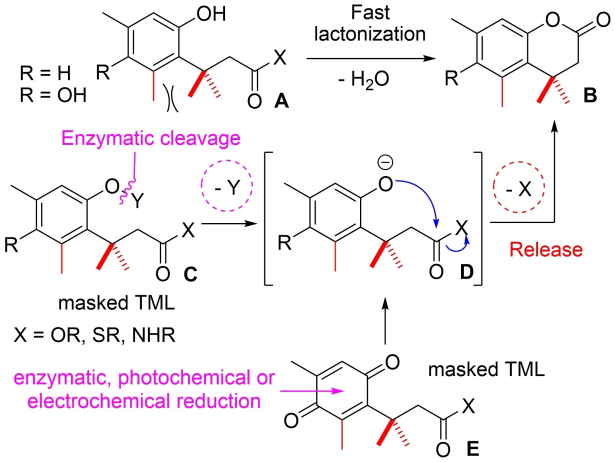

Scheme 1. Principle of the molecular release of TML systems.[1]

[a] C. C. Jimidar, Prof. Dr. J. Grunenberg, Dr. P. Klahn
Institute of Organic Chemistry
Technische Universität Braunschweig
Hagenring 30, 38106 Braunschweig (Germany)
E-mail: p.klahn@tu-braunschweig.de
[b] B. Karge, Dr. H. L. S. Fuchs, Prof. Dr. M. Brönstrup
Department Chemical Biology
Helmholtz Center for Infection Research
Inhoffenstraße 7, 38124 Braunschweig (Germany)
[c] B. Karge, Dr. H. L. S. Fuchs, Prof. Dr. M. Brönstrup
German Center for Infection Research (DZIF) -
Partner site Braunschweig-Hannover (Germany)

Supporting information for this article is available on the WWW under https://doi.org/10.1002/chem.202103525

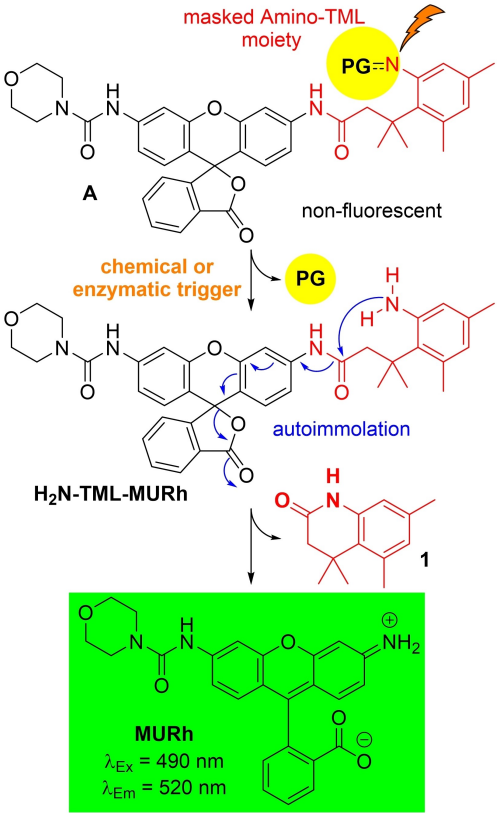

Scheme 2. Principle of masking and molecular release of amino trimethyl lock (H_2N-TML) turn-on fluorescent dyes. PG refers to a protective group (e.g. $-NO_2$, $-N_3$, peptides or azo benzenes), masking H_2N-TML's lactamization reactivity.

bioresponsive smart materials, modern drugs or cell imaging.[1,2] Considering the tremendous success of classical masked TMLs for molecular release systems, we envisaged that novel masked amino trimethyl lock (H_2N-TML) systems based on *ortho*-amino dihydro cinnamic acid derivatives could further broaden the scope of enzymes or chemical triggers applicable for the release of compounds.

To prove our hypothesis that *ortho*-amino dihydro cinnamic acid derivatives can serve as auto-immolative moieties for molecular release of compounds, we planned to synthesize morpholino urea rhodamine (**MURh**) *N*-acylated with masked H_2N-TML moieties (**A**, Scheme 2). *N*-Acylation of this dye is known to quench its fluorescence,[18–22] thus resulting in a turn-on-fluorophore, releasing the parent fluorophore **MURh** upon chemical or enzymatic demasking towards the free **H_2N-TML-MURh** and auto-immolative lactamization of the H_2N-TML moiety under release of dihydroquinolin-2(1H)-one **1**.

For proof of principle of this concept, we synthesized **N_3-TML-CO_2H** (Scheme 3) representing an H_2N-TML masked with an azido moiety, which was supposed to release the corresponding H_2N-TML upon *Staudinger* reduction of azide. Starting from commercially available 3,3-dimethyl acrylic acid (**2**) and 3,5-dimethylaniline (**3**), amide **4** was formed in the presence of thionyl chloride and triethylamine at 80 °C in 91 % yield, which could be converted by an intramolecular *Friedel-Crafts* alkylation in the presence of aluminum trichloride into the dihydroquinolin-2(1H)-one **1** in 97 % yield. The installation of a *tert*-butyl carbamoyl moiety at the nitrogen led to formation of compound **5**, which allowed the saponification of the amide in the presence of aqueous lithium hydroxide solution to obtain the

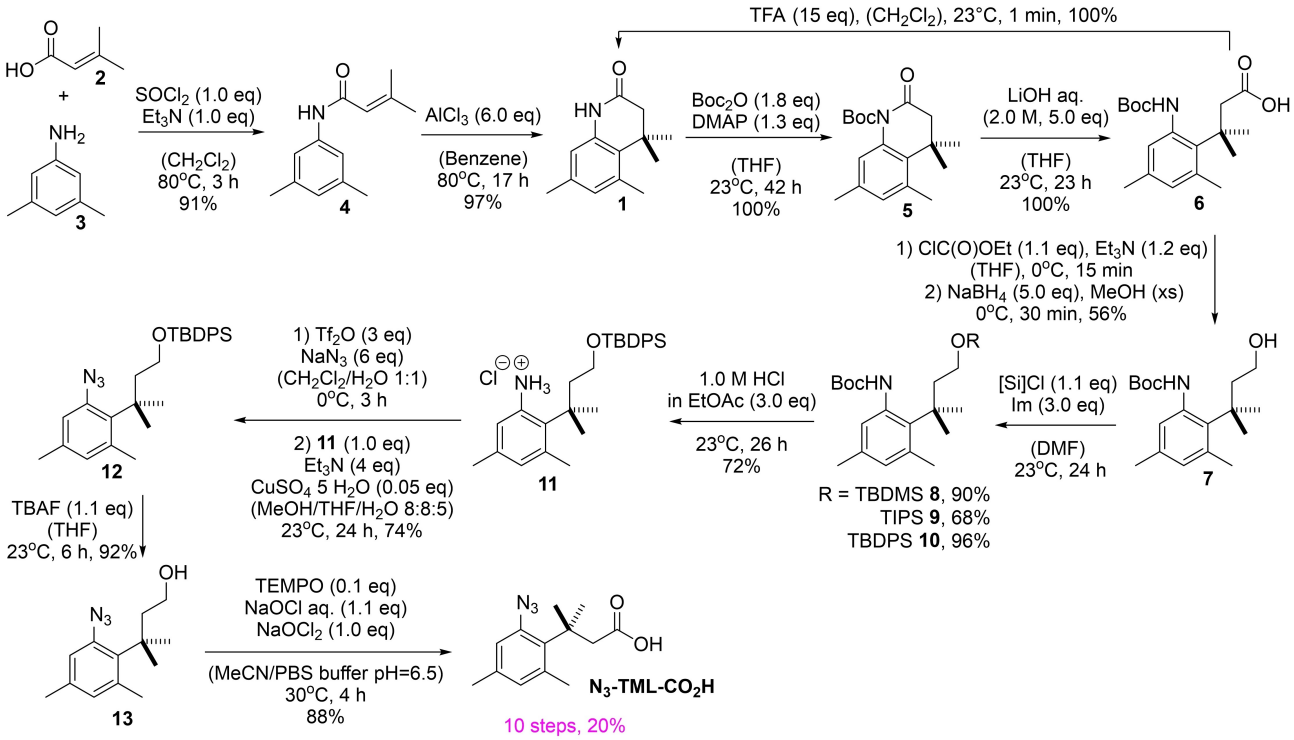

Scheme 3. Synthesis of **N_3-TML-CO_2H**. Abbreviations: Im = 1H-imdazole, xs = excess of the reagent.

N-Boc-protected H_2N-TML-CO_2H **6** in quantitative yield over both steps.

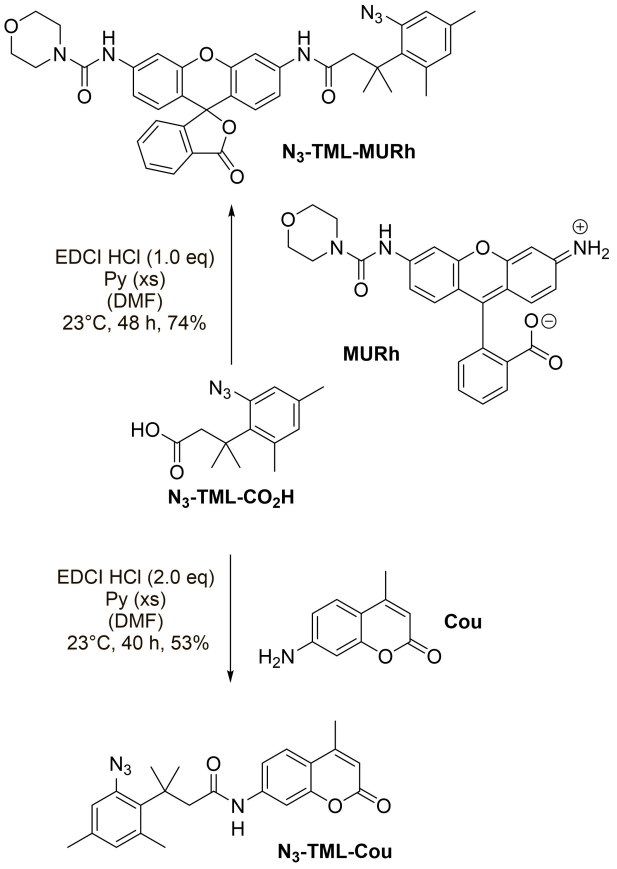

Scheme 4. Synthesis of **N_3-TML-MURh** and **N_3-TML-Cou**. Abbreviations: xs = excess of the reagent.

First evidence for a fast and clean lactamization of the free H_2N-TML-CO_2H was found by the quantitative conversion of **6** into dihydroquinolin-2(1H)-one **1** within less than 1 min in the presence of an excess of TFA in dichloromethane. The carboxylic acid moiety of **6** was then activated in the presence of ethyl chloro formiate and triethyl amine and subsequently reduced with sodium borohydride in the presence of methanol to obtain the *N*-Boc-protected H_2N-TML-alcohol **7** in a moderate yield of 57%. Different silyl protection groups were installed, however, only TBDPS was stable enough to allow a selective deprotection of the Boc group in the presence of 1.0 M HCl in dry EtOAc, yielding the anilinium chloride **11** in 72% yield. A diazotation of the aniline with triflyl azide in the presence of catalytic amounts of copper(II) sulfate gave the azide **12** in 74% yield. Alternatively, the *Goddard-Borger* reagent,[23] a bench stable and safe diazotation reagent, led to slightly decreased yield of 65%. Finally, deprotection of the TBDPS group in the presence of TBAF and subsequent one-pot oxidation in the presence of sodium hypochlorite, sodium chlorite and catalytic amounts of TEMPO led to the formation of the desired **N_3-TML-CO_2H** in 20% overall yield over 10 steps.

With **N_3-TML-CO_2H** in hand, we synthesized **N_3-TML-MURh** (Scheme 4) by *N*-acylation of **MURh** in the presence of EDCI and pyridine as a first turn-on fluorophore, which should release the parent **MURh** upon *Staudinger reduction* of the azide moiety and subsequent auto-immolative lactamization. In similar manner, **N_3-TML-Cou** (Scheme 4) was generated by *N*-acylating 7-amino-4-methylcoumarine (**Cou**). **N_3-TML-Cou** showed only very weak blue fluorescence at an excitation wavelength of $\lambda_{Ex} = 366$ nm, while **N_3-TML-MURh** was practically non-fluorescent (Scheme 5). When both compounds, **N_3-TML-Cou** and **N_3-TML-MURh**, were reacted under *Staudinger* reduction conditions in the presence of triphenylphosphine and acetic acid in a THF/water mixture, the occurrence of a strong blue and green

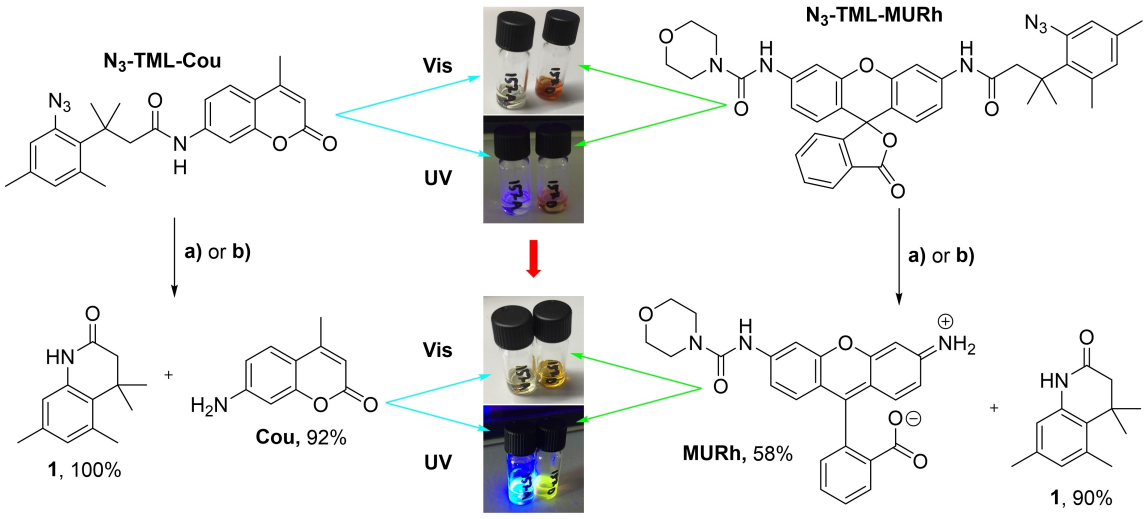

a) PPh_3 (1.0 eq), HOAc (1.0 eq), (THF:H_2O/3:1), 23°C, 5 min.
b) TCEP (100 mM), (50 mM, PBS buffer, pH 7.4), 23°C, 2 min.

Scheme 5. Proof of principle for the turn-on fluorophores **N_3-TML-Cou** and **N_3-TML-MURh**: Release of the fluorophores **Cou** and **MURh** in the presence of PPh_3 or TCEP. UV = Exitation at 366 nm. Pictures show response under condition **a)**.

fluorescence, respectively, was observed within the first 2 min after addition of the triphenylphosphine, clearly indicating the release of the parent fluorophores (Scheme 5). Both parent dyes **Cou** and **MURh** as well as the dihydroquinolin-2(1H)-one **1** have been isolated from the reaction mixtures and identified by TLC-MS as well as ^{1}H NMR.

In addition, when **N_3-TML-Cou** and **N_3-TML-MURh** were dissolved in PBS buffer at pH 7.4, the release of the parent fluorophores could also be achieved in the presence of the water-soluble tris(2-carboxyethyl)phosphine (TCEP) within 2 min at 23 °C (see Supporting Information Figure S4).

Observing the fast fluorescence turn on during the conversion of **N_3-TML-Cou** and **N_3-TML-MURh** and considering the short reaction time for lactamization of **6** (Scheme 3) under acidic and aqueous conditions, we applied systematic conformational analysis and intrinsic reaction path following techniques at the density functional level of theory (wB97XD/6-311+G**//wB97XD/6-31G*) using an implicit water solvent model in order to predict the relative rate constants for both the TML lactonization and the lactam ring closures. As early as 1987 *Houk* and co-workers applied Hartree-Fock theory and limited molecular models, namely *isolated* hydroxy acids in the gas phase, in order to develop the relevant force field parameter, which the authors in a second step used to study a variety of different hydroxy acids.[24] Adapting those molecular models in 2009, *Karaman* used semiempirical AM1 and empirical MM2 calculations to study the thermodynamic and kinetic parameters for pharmaceutically relevant trimethyl lock systems in hydroxy hydro cinnamic acids.[25] Many of these earlier studies were hampered by the fact that, based on both inevitably simplified wave functions *and* the underlying molecular models, a lot of assumptions concerning the real structure and energy of the transition state had to be made. *Houk* and co-workers simply assumed that the Hartree-Fock/3-21G results, especially the predicted O to C distance (2.05 Å) of the "tetrahedral complex" in the gas phase, were similar to that of the transition state in solution.

In our computational study we therefore focused on the unique localization of the relevant transition structures in order to predict the relative rate constants of both lactonization and lactamization reactions, that means the transition structures of the ring closures, if we assume this step to be rate determining.

Starting with an OH to C=O distance of 2.05 Å as proposed by the studies of *Houk* and *Karaman*, but applying DFT theory embedded in a standard continuum solvent model, we nevertheless could not localize any transition structure at all. Even in the case of a protonated carbonic acid, the reaction path is repulsive, preventing any tetrahedral intermediate. Due to our DFT simulations the esterification and lactamization go through a real transition state (Figure 1, A) only if the process is modeled as synchronous C–O (C–N) bond formation in combination with a proton abstraction (Please see animation: C-O.gif and C–N.gif in the Supporting Information Material). However, with a calculated activation barrier of $>$42.0 kcal/mol (lactonization) and $>$44.0 kcal/mol (lactamization) this trajectory appears to be very unlikely even at high temperature. As expected, the protonation of the carboxylic oxygen leads to a lower (Figure 1,

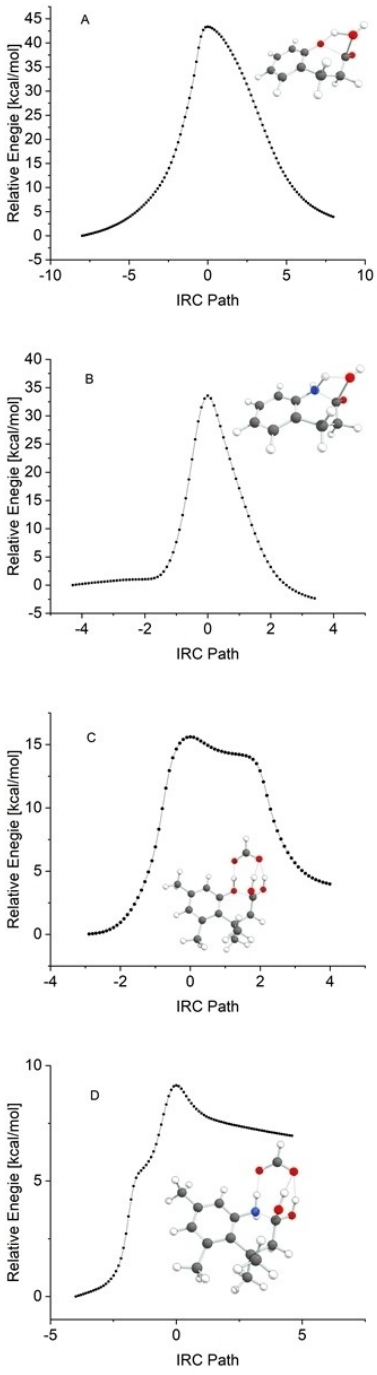

Figure 1. Intrinsic reaction path of several intramolecular lactonization/lactamization reactions calculated at the ωB97X–D/dz level of theory (see text). The insets depict the computed transition state structures, respectively. A: Reaction path of phenolic lactonization (without TML). The process is modeled as a synchronous C–O bond formation in combination with proton abstraction (see animation CO.gif in Supporting Information). Note the high activation barrier of around 40 kcal/mol. B: The analogue IRC path of the lactamization" (again, without TML, see animation CN.gif in Supporting Information). C: Reaction path of lactonization with proton shuttle: an additional carboxylic moiety, simplified as a formic acid, was included in our simulation. The activation barrier is low (around 15 kcal/mole). D: Reaction path of the analogue lactamization including formic acid as a proton shuttle with an even lower barrier of 10 kcal/mol.

B), but still substantial barrier of ~35 kcal/mol (Please see the animation for the amino case: C–N-protonated.gif in the Supporting Information). Though, due to our calculations this substantial barrier is reduced by the physical presence of the TML groups in our molecular models (Barrier with TML: 35.1 kcal/mol and 36.2 kcal/mol for the lactonization and the lactamization, respectively) these values are still not compatible with the experimentally well documented facility of this reaction.

In order simulate the condensed phase is a more realistic way, and adapting the well-known property of carboxylic acids to form dimers, we, in a second step, included one additional carboxylic moiety (simplified as a formic acid) in our molecular computer models. Due to our calculations the second hydroxy acid moiety plays the key role in both the lactone and the lactam cyclization, namely as a proton shuttle.

Starting with our dimeric hydroxy-acid educt (O to C distance: 2.42 Å), while perfectly pre-organized ("proximity effect"), showing only weak, non-covalent O–C interactions (Force constant: +0.4 N/cm), the protonation of the carboxyl oxygen is connected with a pronounced "shoulder" visible in the reaction coordinate. Nevertheless, only after the onset of the hydroxy deprotonation, the "true" transition state connected with a forming C–O bond (O–C force constant: −1.6 N/cm) is reached (please see animation: Lacton.gif in the Supporting Information Material). Most importantly, the barrier height (strictly enthalpic!) of the overall ring closure step is reduced to a value below 12 kcal/mol (Figure 1, C), making our simulation model much more realistic in comparison with the mono-molecular mechanism. The proton shuttle mechanism changes in the H_2N-TML system: In this case, starting with our amino-acid educt (N to C distance: 2.40 Å, force constant: +0.5 N/cm), the protonation of the carboxyl oxygen succeeds the lactam ring closure, making the overall process (concerning again "only" the enthalpy) virtually barrierless (Figure 1, D). In contrast to the mono-molecular mechanism assumed by *K. Houk* and others for the ring closure step in prototypical lactonizations and lactamizations, our computed bi-molecular proton shuttle mechanism is self-catalytical by nature. The carbonic acid in our computation represents just a truncated model for a second starting material molecule. Next, we investigated whether the release of the parent fluorophores from **N_3-TML-Cou** and **N_3-TML-MURh** could also be triggered by other conditions than the presence of phosphines. Although the cleavage of both compounds could at least partially be achieved photolytically by irradiation at 360 nm, the overall quantum yield and conversion seemed to be very low and decomposition of the probes was an issue.

However, we were delighted to see that both **N_3-TML-Cou** and **N_3-TML-MURh** responded to physiological conditions of hydrogen sulfide (H_2S) by the release of their parent fluorophore (Figure 2). While **N_3-TML-Cou** was reacting much faster in the presence of H_2S at 100 μM concentration, reaching the maximum fluorescence emission after 60 min (Figure 2A), **N_3-TML-MURh** showed an overall slower conversion and release of the parent fluorophore **MURh** under the same conditions (Figure 2B).

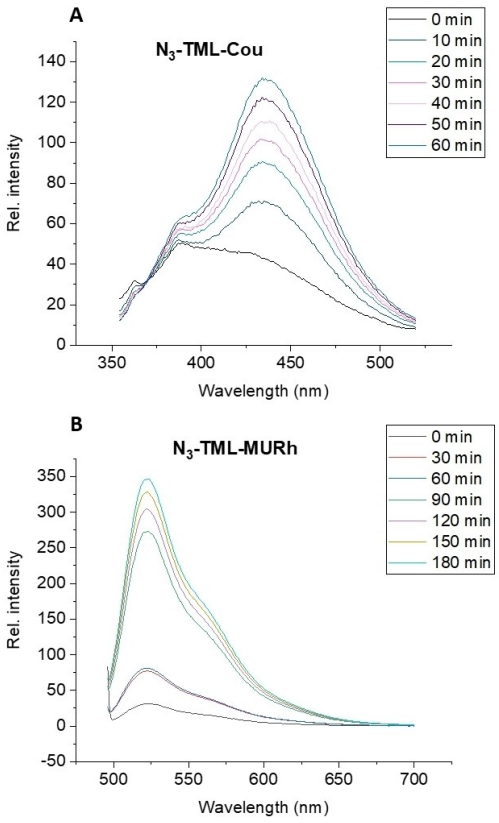

Figure 2. A) Relative intensity of the fluorescence emission spectrum of **N_3-TML-Cou** (10 μM) in aqueous PBS buffer (50 mM, pH = 7.4 with 0.2% DMSO) after treatment with Na_2S (100 μM, 50 mM PBS buffer pH = 7.4) at 37 °C at different time points. B) Relative intensity of the fluorescence emission spectrum of **N_3-TML-MURh** (10 μM) in aqueous PBS buffer (50 mM, pH = 7.4 with 0.2% DMSO) after treatment with Na_2S (100 μM, 50 mM PBS buffer pH = 7.4) at 37 °C at different time points.

H_2S is an important gaseous signaling molecule playing numerous roles in healthy metabolism of human,[26,27] plant[28] and bacterial[29] cells and is involved in several physiological processes such as the regulation of the intracellular redox status, neuronal transmission or the relaxation of smooth muscles, but also plays a central role in the pathophysiology of different diseases.[27,30] Therefore, cellular detection of H_2S by fluorescent probes is of high interest[31–34] and azide-based probes for this purpose have been described earlier.[35] However, an important criterium for the proper imaging of H_2S levels is a good selectivity of the probe for the detection of H_2S in the presence of multiple other biological sulfur species such as cysteine, glutathione (GSH), or lipoic acid (LA).[27,33] Therefore, we explored the selectivity of both probes in the presence of a variety of different reactive sulfur and nitrogen species known to be present in human tissue (Figure 3). Despite the relatively high fluorescence background, **N_3-TML-Cou** displayed a significant response to H_2S, cysteine and glutathione, while its response to lipoic acid, nitrite, thiosulfate, dithionite, thiocyanate and sulfite was less pronounced (Figure 3A). To our delight, **N_3-TML-MURh** showed a very selective response to H_2S,

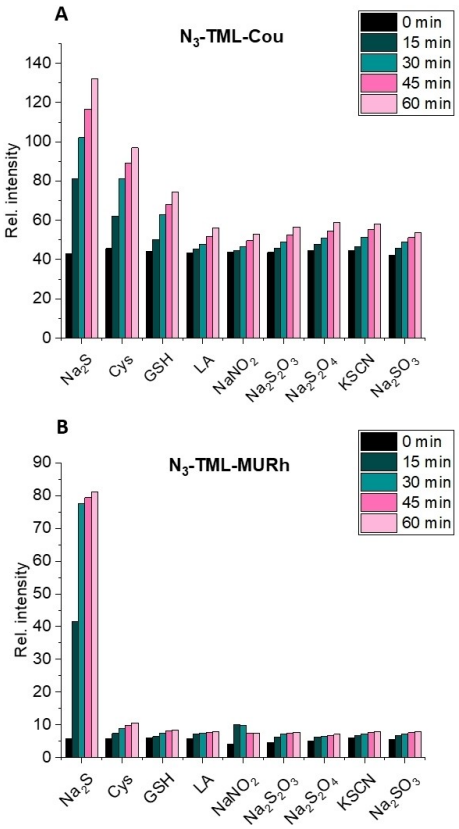

Figure 3. Selectivity profile of **N_3-TML-Cou** (A) and **N_3-TML-MURh** (B) towards reactive sulfur and nitrogen species. From left to right: 100 μM Na_2S, 5 mM L–Cysteine, 5 mM Glutathione (GSH), 100 μM Lipoic acid (LA), 100 μM $NaNO_2$, 100 μM $Na_2S_2O_3$, 100 μM $Na_2S_2O_4$, 100 μM KSCN, 100 μM Na_2SO_3. Conditions: A) 10 μM **N_3-TML-Cou**, PBS buffer (50 mM, pH = 7.4). λ_{ex} = 343 nm, λ_{em} = 444 nm incubated at 37 °C. B) 10 μM **N_3-TML-MURh**, PBS buffer (50 mM, pH = 7.4). λ_{ex} = 492 nm, λ_{em} = 529 nm incubated at 37 °C.

while the presence of all other reactive sulfur and nitrogen species led to negligible fluorescence.

However, the significantly better selectivity of **N_3-TML-MURh** comes at the cost of a much higher detection limit compared to **N_3-TML-Cou**. While the H_2S detection limit of **N_3-TML-MURh** was determined to be 100 μM in vitro (Figure S7 in the Supporting Information), **N_3-TML-Cou** gave already a fluorescent response at 0.1 μM concentration of H_2S. However, as normal physiological concentrations of H_2S in healthy tissue and serum cover ranges between 30–300 μM and diseases associated concentrations can reach up to 600 μM,[36] less sensitive but highly selective probes like **N_3-TML-MURh** seemed to be well suited for the detection of H_2S in cells. Inspired by these results, we next aimed to investigate the ability of **N_3-TML-MURh** to visualize H_2S in mammalian cells by fluorescence microscopy. For this purpose, adherent human embryonic kidney (HEK293T) cells were incubated with **N_3-TLM-MURh** and subsequently treated with Na_2S (50 μM) for 45 min at 37 °C (Figure 4). **N_3-TML-MURh** induced a clear fluorescent signal, which seems to show a localization at mitochondria and the endoplasmic reticulum (ER) of the cells (Figure 4B and D).[37] This signal was sulfide-dependent, as the negative control in

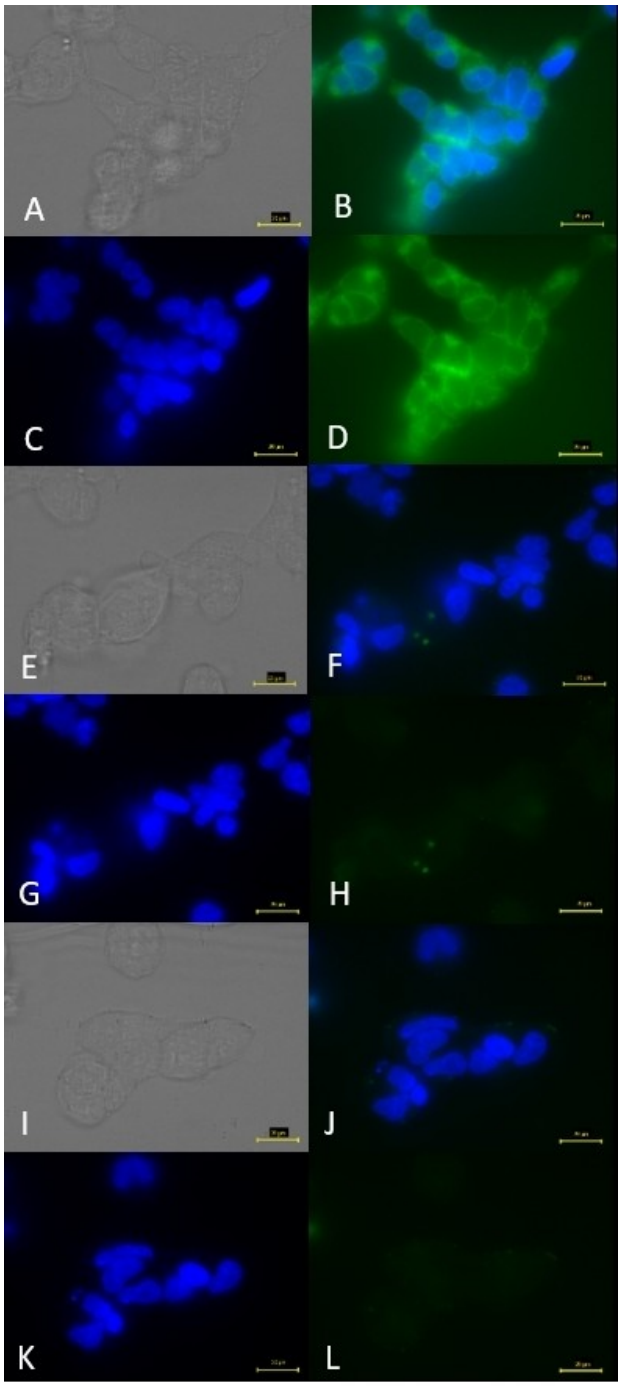

Figure 4. Detection of H_2S by fluorescence microscopy in HEK293T cells. (A–D) Images with **N_3-TLM-MURh** (200 μM) following incubation with Na_2S (50 μM, 45 min). A) Brightfield image, B) merged fluorescence images, C) cell nuclei stained with Hoechst, D) H_2S visualized by **N_3-TLM-MURh**. (E–H) Negative control: Images with **N_3-TLM-MURh** (200 μM), but in absence of Na_2S. E) Brightfield image, F) merged fluorescence images G) cell nuclei stained with Hoechst, H) **N_3-TLM-MURh**. (I–L) Negative control: Images with **N_3-TLM-MURh** (200 μM), cell preincubated with $ZnCl_2$ (1 mM), following incubation with Na_2S (50 μM, 45 min). I) Brightfield image, J) merged fluorescence images, K) cell nuclei stained with Hoechst, L) **N_3-TLM-MURh**. Yellow scalebars = 20 μm.

absence of Na_2S was non-fluorescent (Figure 4F and H). Likewise, when the sulfide ions were removed by pre-incubation of the cells with $ZnCl_2$,[38] no fluorescent signal was detected upon treatment of the cells with **N_3-TLM-MURh** (Figure 4J and L). These experiments demonstrate that **N_3-TLM-MURh** is cell-permeable and capable to visualize H_2S in a cellular context.

In summary, we designed two turn-on fluorophores based on a novel azide-masked H_2N-TML moiety suitable to enable the release of different fluorophores upon chemical or bio responsive demasking. Furthermore, our computations suggest that the fast auto-immolative lactamization proceeds via an almost barrierless bi-molecular mechanism with an external proton shuttle. **N_3-TML-MURh** was demonstrated to selectively respond to physiological concentrations of the important gaseous signaling molecules H_2S by release of highly fluorescent **MURh** and proven suitable for H_2S imaging in an in vitro cell culture model. Compared to other non-activatable probes, the N_3-TML system offers the advantage for application to H_2S-responsive prodrug approaches, as the **N_3-TML-CO_2H** moiety could also be utilized to mask the heteroatoms (N, O, S atoms) of drugs or other effectors. To underline the potential of masked H_2N-TML for the development of turn-on fluorophores and applications in drug delivery concepts, we are currently investigating the installation of enzymatically cleavable masking groups at the H_2N-TML moiety as well as working on the development of targeted drug conjugates bearing H_2S-responsive linkers based on N_3-TML systems.

Experimental Section

Experimental details can be found in the Supporting Information.

Author Contributions

The research was conceived by P.K. The manuscript was written by P.K., J.G. and M.B. All compounds were synthesized by C.C.J. and P.K. Supporting Information were prepared by C.C.J., B.K., H.F. and P.K. Computations were planned and conducted by J.G. Fluorescence spectroscopy and SRS selectivity studies were planned by P.K. and C.C.J. and conducted by C.C.J. Fluorescence microscopy and imaging studies on cells were planned by M.B., P.K., H.F. and B.K., and conducted by B.K. All authors have given approval to the final version of the manuscript.

Acknowledgements

This work has been carried out within the framework of the SMART BIOTECS alliance between the Technische Universität Braunschweig and the Leibniz Universität Hannover. This initiative is supported by the Ministry of Science and Culture (MWK) of Lower Saxony, Germany. Financially support by the DFG (Grant KL3012/2-1) and Fonds der Chemischen Industrie the is gratefully acknowledged. The content of this work is solely the responsibility of the authors and does not necessarily represent the official views of the funding agencies. The authors thank Carina P. Glindemann for support in the synthesis of **N_3-TML-CO_2H**, Bettina Hinkelmann for support with the cellular imaging experiments, the mass spectrometry unit, in particular Dr. Ulrich Papke, and the NMR spectroscopy unit of the Institute of Organic Chemistry, in particular Dr. Kerstin Ibrom, for analytical support. We furthermore thank Dr. Anna Luisa Klahn for helpful discussion and proofreading of the manuscript. Open Access funding enabled and organized by Projekt DEAL.

Conflict of Interest

The authors declare no conflict of interest.

Keywords: H_2S imaging · lactams · molecular release · trimethyl lock · turn-on fluorescence

[1] O. A. Okoh, P. Klahn, *ChemBioChem* **2018**, *19*, 1668–1694.
[2] M. N. Levine, R. T. Raines, *Chem. Sci.* **2012**, *3*, 2412.
[3] P. T. Wong, S. K. Choi, *Chem. Rev.* **2015**, *115*, 3388–3432.
[4] A. Alouane, R. Labruère, T. Le Saux, F. Schmidt, L. Jullien, *Angew. Chem. Int. Ed.* **2015**, *54*, 7492–7509; *Angew. Chem.* **2015**, *54*, 7492–7509.
[5] A. S. Skwarecki, S. Milewski, M. Schielmann, M. J. Milewska, *Nanomed. Nanotechnol. Biol. Med.* **2016**, *12*, 2215–2240.
[6] P. Klahn, V. Fetz, A. Ritter, W. Collisi, B. Hinkelmann, T. Arnold, W. Tegge, K. Rox, S. Hüttel, K. I. Mohr, J. Wink, M. Stadler, J. Wissing, L. Jänsch, M. Brönstrup, *Chem. Sci.* **2019**, *10*, 5187–5425.
[7] P. Klahn, M. Brönstrup, *Nat. Prod. Rep.* **2017**, *34*, 832–885.
[8] B. Nolting, in *Antibody-Drug Conjugates Methods Molecular Biology* (Ed.: L. Ducry), Humana Press, Totowa, NJ, **2013**, pp. 51–70.
[9] J. D. Bargh, A. Isidro-Llobet, J. S. Parker, D. R. Spring, *Chem. Soc. Rev.* **2019**, *48*, 4361–4374.
[10] R. Liu, P. A. Miller, S. B. Vakulenko, N. K. Stewart, W. C. Boggess, M. J. Miller, *J. Med. Chem.* **2018**, *61*, 3845–3854.
[11] X. Zhang, X. Li, Q. You, X. Zhang, *Eur. J. Med. Chem.* **2017**, *139*, 542–563.
[12] R. Walther, J. Rautio, A. N. Zelikin, *Adv. Drug Delivery Rev.* **2017**, *118*, 65–77.
[13] D. Shan, M. G. Nicolaou, R. T. Borchardt, B. Wang, *J. Pharm. Sci.* **1997**, *86*, 765–767.
[14] J. Rautio, N. A. Meanwell, L. Di, M. J. Hageman, *Nat. Rev. Drug Discovery* **2018**, *17*, 559–587.
[15] G. G. Dias, A. King, F. de Moliner, M. Vendrell, E. N. da Silva Júnior, *Chem. Soc. Rev.* **2018**, *47*, 12–27.
[16] J. Yan, S. Lee, A. Zhang, J. Yoon, *Chem. Soc. Rev.* **2018**, *47*, 6900–6916.
[17] S. Milstien, L. A. Cohen, *Proc. Nat. Acad. Sci.* **1970**, *67*, 1143–1147.
[18] M. N. Levine, R. T. Raines, *Anal. Biochem.* **2011**, *418*, 247–252.
[19] L. D. Lavis, T. Chao, R. T. Raines, *ACS Chem. Biol. Biol* **2006**, *1*, 252–260.
[20] L. D. Lavis, T. Y. Chao, R. T. Raines, *ChemBioChem* **2006**, *7*, 1151–1154.
[21] M. M. Yatzeck, L. D. Lavis, T. Y. Chao, S. S. Chandran, R. T. Raines, *Bioorg. Med. Chem. Lett.* **2008**, *18*, 5864–5866.
[22] W. C. Silvers, A. S. Payne, R. L. McCarley, *Chem. Commun.* **2011**, *47*, 11264.
[23] E. D. Goddard-Borger, R. V. Stick, *Org. Lett.* **2007**, *9*, 3797–3800.
[24] A. E. Dorigo, K. N. Houk, *J. Am. Chem. Soc.* **1987**, *2157*, 5404.
[25] R. Karaman, *Bioorg. Chem.* **2009**, *37*, 11–25.
[26] H. Kimura, *Nitric Oxide - Biol. Chem.* **2014**, *41*, 4–10.
[27] G. K. Kolluru, X. Shen, S. C. Bir, C. G. Kevil, *Nitric Oxide - Biol. Chem.* **2013**, *35*, 5–20.
[28] A. Caverzan, L. A. Ebone, J. L. T. Chiomento, G. Chavarria, *Arch. Agron. Soil Sci.* **2021**, *00*, 1–13.
[29] K. Shatalin, E. Shatalina, A. Mironov, E. Nudler, *Science* **2011**, *334*, 986–990.
[30] N. Yang, Y. Liu, T. Li, Q. Tuo, *DNA Cell Biol.* **2020**, *39*, 187–196.
[31] H. Li, Y. Fang, J. Yan, X. Ren, C. Zheng, B. Wu, S. Wang, Z. Li, H. Hua, P. Wang, Z. Li, H. Hua, P. Wang, D. Li, *TrAC Trends Anal. Chem.* **2021**, *134*, 116117.
[32] L. Zhou, Y. Chen, B. Shao, J. Cheng, X. Li, *Front. Chem.* **2021**, 1–30.

[33] H. Ibrahim, A. Serag, M. A. Farag, *J. Adv. Res.* **2021**, *27*, 137–153.
[34] H. Peng, W. Chen, Y. Cheng, L. Hakuna, R. Strongin, B. Wang, *Sensors (Switzerland)* **2012**, *12*, 15907–15946.
[35] V. S. Lin, A. R. Lippert, C. J. Chang, *Methods Enzymol.* **2015**, 63–80.
[36] Y. Han, Q. Shang, J. Yao, Y. Ji, *Cell Death Dis.* **2019**, *10*, 293.
[37] C. Guardia-Laguarta, E. Area-Gomez, C. Rub, Y. Liu, J. Magrane, D. Becker, W. Voos, E. A. Schon, S. Przedborski, *J. Neurosci.* **2014**, *34*, 249–259.
[38] L. Zhang, X. E. Zheng, F. Zou, Y. Shang, W. Meng, E. Lai, Z. Xu, Y. Liu, J. Zhao, *Sci. Rep.* **2016**, *6*, 1–10.

Manuscript received: September 28, 2021
Accepted manuscript online: October 29, 2021
Version of record online: November 8, 2021